Advanced Materials Manufacturing & Characterization

journal home page: www.ijammc-griet.com

Haz Formation And Analysis In Flux Assisted Gtaw

Gurveen Singh*, Dinesh Kumar Shukla

Department of Mechanical Engineering, Dr. B.R. Ambedkar National Institute of Technology, Jalandhar. Punjab. India (144011)

ABSTRACT

The effect of Silicon dioxide (SiO_2) powder on weld bead geometry, Heat affected zone (HAZ), and micro-hardness of SS304 grade Austenitic stainless steel weld was investigated. SiO_2 improves the weld bead penetration with a simultaneous reduction in bead width. The improvement in penetration results from arc constriction and reversal of Marangoni flow. The results demonstrate SiO_2 flux can increase the heat density by arc constriction and Marangoni convection. The temperature in HAZ reaches above the recrystallization temperature and consequently leads to the formation of new grains. The new grains formed in HAZ are of a very large size as compared to parent metal grains. Due to Larger grains, the micro-hardness in HAZ area was found to be less than weld metal and base metal zone. Increased heat density by using SiO_2 flux increased the size of Heat Affected Zone.

Keywords- Active TIG, Marangoni convection, arc constriction, HAZ

INTRODUCTION - Gas Tungsten arc welding (GTAW) process or Tungsten Inert Gas (TIG) Welding Process uses a non-consumable tungsten electrode to generate an electric arc for fusion of work-pieces[1]. The electrode is protected with inert gas generally argon or helium to prevent oxidation at high temperature. This process is highly used for good quality welds of stainless steel, alloy steels, magnesium and aluminum alloys[2]. However, the process lacks in achieving penetration greater than 3mm. Full fusion joints are made by V-Groove edge preparations and multi-pass welding procedures which reduce the productivity of process[3]. There was a definite need to improve the penetration of process. The problem of poor penetration and thereby low productivity was overcome by using activated flux.

Paton Institute in the 1960s developed the activated flux for improving weld bead penetration[4]. This technique gained the interest of researchers from the year 2000 onwards to improve weld bead geometry [5]. In this technique, active flux made of oxide powders is mixed with a thinner like acetone or ethanol to have a paint-like consistency. It is applied to the base metal before welding as shown in Fig-1. At high temperature during welding, oxygen decomposes from the oxide powders[6]. Oxygen being a surface active element reverses the Marangoni flow to improve weld bead geometry [7].

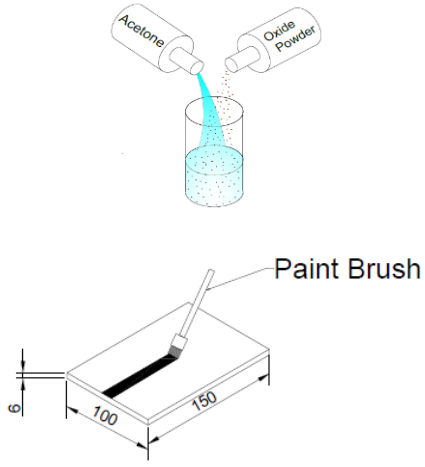

a) Mixing b) Coating

Fig -1 Application of Active flux

Several researchers had worked on using active flux made of oxide powders like SiO_2, ZnO, TiO_2, Fe_2O_3 and

• Corresponing author Gurveen Singh,E-mail address: gurveensingh03@gmail.com
• Doi: http://dx.doi.org/10.11127/ijammc2018.09.01

reported more than 100% increase in depth of penetration on ferrous and nonferrous materials. Metallurgical and mechanical properties of the welded joints had also improved with the use active flux [8], [9]. The process is generally known as Active TIG Welding Process (A-TIG) [10]. However, less work has been reported on the formation of HAZ and its effect on the metallurgical and mechanical properties of the material. This paper presents the formation and analysis of HAZ on the important aspects of activated TIG welded joint.

Mechanisms of penetration improvement

Two mechanisms viz Marangoni convection and arc constriction are most commonly adopted for explaining the improvement of penetration in flux assisted GTAW process. Marangoni convection states that fluid flow is controlled by surface tension gradient. Fluid flows from the region of lower surface tension to the region of higher surface tension[11]. Oxygen decomposes from the oxide powders at high temperature and being a surface active element for ferrous materials, it changes the surface tension driven flow[12]. Initially, the surface tension was higher at the edge of the weld pool and lower at the center. With the presence of oxygen in the weld pool, the surface tension gradient of the weld pool reverses and surface tension becomes higher at center and lower at the edge of weld pool[13]. This reversal of surface tension flows the liquid metal down rather than outward flow as shown in Fig 2. Many researchers had used this phenomenon to explain the improvement in penetration obtained by use of active flux powders[14].

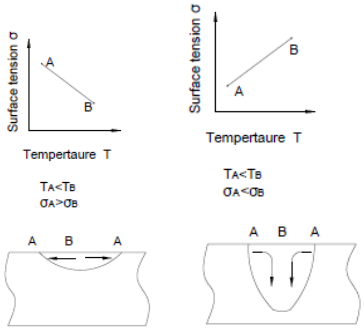

Fig 2-Marangoni Flow: a) Without Active Flux b) With Active Flux [15]

Some of the researchers captured images of arc during welding with and without active flux. They observed constriction in an arc when active flux was used in welding[16]. Arc constriction was attributed to the electronegativity of ions of the active element present in weld pool [17]. When weld pool contains sufficient amount of active element, the arc column diameter reduces thereby increasing the heat density or the anode root area thus leading to enhancement of weld penetration as shown in Fig 3.

Welding Condition	Arc Column	Weld Bead obtained
Without Flux	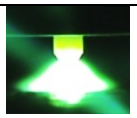	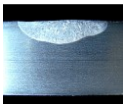
With SiO_2 Flux	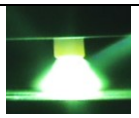	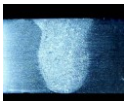

Fig 3-Arc image and weld bead geometry obtained in two different welding conditions[18]

Heat Affected Zone

Heat affected zone is an area of base metal adjacent to weld metal which is affected by intense heat and undergoes metallurgical changes. This change of metallurgical behavior of very important to study as it can change the mechanical properties of the welded joint [19], [20]. HAZ area of the base metal can increase or decrease depending on heat input rate. Active flux increases the heat flux by arc constriction and Marangoni convection; hence its effect on HAZ formation needs to be studied. This paper presents the effect of SiO_2 flux assisted GTAW process on the metallurgical behavior and HAZ formation on SS-304 grade austenitic stainless steel.

EXPERIMENTATION

A direct current, electrode negative polarity power source (EWM-Tetrix 351) was used with an automated system in which the specimen was moved at a constant speed while keeping the torch fixed. A water-cooled torch with 2% thoriated tungsten electrode of diameter 2.4 mm was used in this study. Electrode vertex angle of 30^0, Electrode to workpiece distance of 2mm and electrode extension of 3 mm was kept fixed for all experiments. Argon was selected as the inert gas to protect the weld region from atmospheric contamination.

Austenitic stainless steel SS-304 grade was selected for this study as this is the most commonly used grade of stainless steel. The chemical composition of the SS-304 grade is given in Table-1. The test specimens were

prepared with the dimensions of 100 x 150 mm with 6mm thickness. The surface of metallic plates was cleaned with 100 grit size abrasive paper to remove all surface impurities and was further cleaned with acetone before welding.

Table -1 Chemical Composition of SS-304

Element	C	Cr	Ni	P	S
%age	0.069	18.8	8.02	0.0341	0.0103
	Si	Mo	Cu	Mn	Fe
	0.312	0.242	0.434	0.985	Balance

Active flux was prepared by mixing the SiO_2 powder with acetone in 1:1 ratio to have paint like consistency. It was applied with a paint brush on the weld region before welding. Acetone is a volatile liquid evaporates leaving behind a layer of SiO_2 powder stuck with the base metal. Autogenous bead on plate welds was made in a single pass at 180 A welding current and 2mm/s welding speed keeping all welding variables identical.

After welding, the weld beads were sectioned and the specimens for metallographic testing were prepared by grinding and polishing the specimen. Etching was done by dipping the specimen in a solution of HCl, $CuSO_4$ and distilled water[21]. The weld bead cross-sections were photographed by Leica Microscope at different magnifications. Micro-hardness of the specimens was measured by Vickers hardness testing machine. A high-speed camera was used to record the image of arc column during welding.

RESULTS AND DISCUSSION

Weld Bead geometry and arc column

After Etching, the weld bead was revealed and recorded by using an optical microscope. Weld bead measurement was done with tool maker's microscope. Fig 4 shows the weld beads obtained with and without flux at 5LPM and 15 LPM flow rate of inert gas. There was a significant difference in the weld bead shape obtained with and without SiO_2 Flux. Flux assisted GTA Process has shown a tremendous increment in weld bead depth (D) with a simultaneous reduction in Bead

width (W). The change in penetration is attributed to the reversal of Marangoni convection flow and arc constriction. Full depth penetration of 6mm has been achieved by using SiO2 flux. Arc column images were recorded with a high-speed camera during welding. It was observed that the arc column diameter gets reduced when welding with flux. This constriction of arc increases the heat flux leading to increased weld bead penetration.

Effect on HAZ

Fig 5 exhibits the microstructure of three zones obtained after welding i.e. Weld metal, HAZ and Base Metal. The weld metal zone depicts the formation of skeletal ferrite and lathy ferrite formation in austenite microstructure resulting from primary ferrite solidification[22]. All the welded samples had shown a similar formation of ferrite after solidification of the weld metal. The area adjacent to weld metal is largely affected by heat and is termed as heat affected zone. The temperature in the HAZ reaches above recrystallization temperature and leads to the formation of new grains. The quick solidification of metal leads to the formation of larger sized grains in HAZ as compared to base metal grains. Larger grains can lead to a reduction of micro-hardness, tensile strength, and other mechanical properties.

Flux plays a significant role in deciding the thickness of HAZ. Fig 6 illustrates HAZ formation by welding with and without active flux. When welding without flux, a smaller portion undergoes the change in grain size whereas flux assisted GTA process has shown a larger portion undergoing recrystallization. This increase in the size of HAZ is attributed to the increase in heat flux while using active flux due to arc constriction and Marangoni convection. The increased heat flux leads to a larger zone of parent metal undergoing recrystallization.

Effect on Microhardness

Fig 7 exhibits the micro-hardness values of weld beads prepared with different welding conditions of gas flow rate and flux application. Micro-hardness values were recorded at an interval of 0.5 mm and up to a distance of 8mm from weld bead center to investigate the hardness profile of the weld metal,

Inert Gas Flow Rate	Welding Condition	Weld bead shape	Arc Column Image	Weld Bead Dimensions
5 LPM	Without Flux			D- 3.38 mm, W-9.17 mm
	With SiO_2 Flux		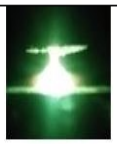	D- 6 mm, W- 6.83mm
15 LPM	Without Flux			D- 4.04 mm, W-7.37 mm
	With SiO_2 Flux			D- 6 mm, W- 5.76mm

Fig 4- Weld bead geometry and Arc column images at different welding conditions

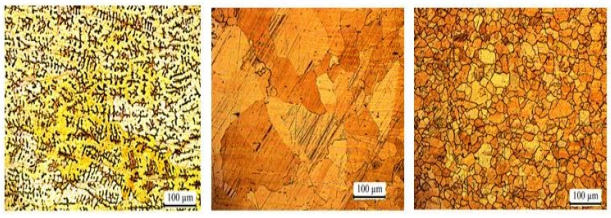

a) b) c)

Fig 5- Microstructure of three zones, a) Weld Metal, b) HAZ, c) Base Metal

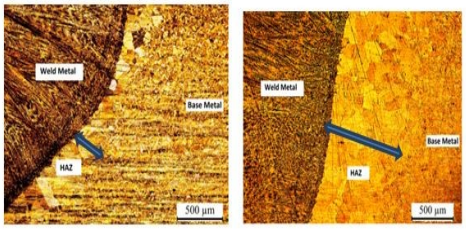

Fig 6- HAZ size a) Without Flux | b) With Flux

heat affected zone and base metal. Micro-hardness values were measured by applying a load of 200 gm with a dwell period of 12 seconds. The average Hardness value of weld metal in all the samples was 180HV. HAZ has been recorded with the least hardness value with the average of 165 HV. Whereas the base metal average hardness of all the sampleswas 200HV. Low hardness value of HAZ zone can be attributed to the coarse grain size formed during solidification and recrystallization of the affected metal

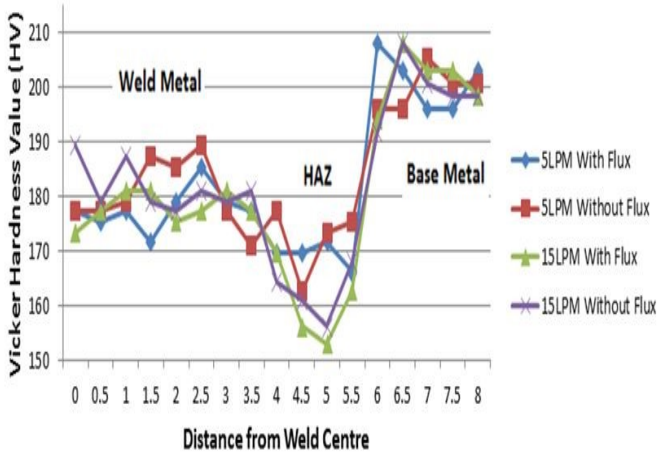

Fig 7 – Microhardness profile at different welding zones

CONCLUSION

1. SiO_2 flux assistance in GTA process significantly improves the weld bead penetration. Full depth penetration welds up to 6mm can be made by applying SiO_2 flux prior to the welding.
2. The HAZ exhibits large grains as compared to base metal grains. These large size grains results from quick solidification and transformation of base metal and can have a deteriorating effect on mechanical properties of the welded joint.
3. SiO_2 flux assisted GTA welds had shown an increase in the size of HAZ. Increased heat density leads to a larger area of base metal undergoing recrystallization.
4. HAZ has been recorded with the least hardness value as compared to weld metal and base metal. The low hardness value has been attributed to the coarse grains formed in HAZ after recrystallization.

REFERENCES

[1] Miller, *Guidelines for Gas Tungsten Arc Welding (GTAW)*. 2017.

[2] Little Richard L, "Welding and Welding Technology," *Mc Graw Hill Education*, p. 1973, 1973.

[3] S. Lu, H. Fujii, and K. Nogi, "Marangoni convection and weld shape variations in He-CO2 shielded gas tungsten arc welding on SUS304 stainless steel," *Journal of Materials Science*, vol. 43, no. 13, pp. 4583–4591, 2008.

[4] H.-Y. Huang, "Effects of activating flux on the welded joint characteristics in gas metal arc welding," *Materials & Design*, vol. 31, no. 5, pp. 2488–2495, 2010.

[5] D. S. Howse and W. Lucas, "An Investigation into arc constriction by active fluxes for tungsten inert gas welding," *Science and Technology of Welding and Joining*, vol. 5, no. 3, pp. 189–193, 2000.

[6] K. H. Tseng, "Development and application of oxide-based flux powder for tungsten inert gas welding of austenitic stainless steels," *Powder Technology*, vol. 233, pp. 72–79, 2013.

[7] J. Niagaj, "Effect of A-TIG welding on deformation of austenitic steel components," *Welding International*, no. July 2014, pp. 1–4, 2011.

[8] R. S. Vidyarthy, D. K. Dwivedi, and M. Vasudevan, "Optimization of A-TIG Process Parameters Using Response Surface Methodology," *Materials and Manufacturing Processes*, vol. 6914, no. March, 2017.

[9] G. R. Kumar, G. D. J. Ram, and S. R. K. Rao, "Microstructure and mechanical properties of borated stainless steel (304B) GTA and SMA welds," *Metallurgia Italiana*, vol. 107, no. 5, pp. 47–52, 2015.

[10] A. Rodrigues, A. Loureiro, A. Rodrigues, and A. Loureiro, "Effect of shielding gas and activating flux on weld bead geometry in tungsten inert gas welding of austenitic stainless steels Effect of shielding gas and activating flux on weld bead geometry in tungsten inert gas welding of austenitic stainless steels," vol. 1718, no. October, 2015.

[11] J. Thomson, "On certain curious Motions observable at the Surfaces of Wine and other Alcoholic Liquors," *The London, Edinburgh and Dublin Philosophical Magazine and Journal of Science*, vol. 10, no. May, p. 330, 1855.

[12] S. Lu, H. Fujii, and K. Nogi, "Marangoni Convection and Gas Tungsten Arc Weld Shape," *ISIJ International*, vol. 46, no. 2, pp. 276–280, 2006.

[13] S. Lu, H. Fujii, and K. Nogi, "Influence of welding parameters and shielding gas composition on GTA weld shape," *ISIJ International*, vol. 45, no. 1, pp. 66–70, 2005.

[14] S. Lu, H. Fujii, H. Sugiyama, M. Tanaka, and K. Nogi, "Weld Penetration and Marangoni Convection with Oxide Fluxes in GTA Welding," *Materials Transactions*, vol. 43, no. 11, pp. 2926–2931, 2002.

[15] S. Lu, H. Fujii, and K. Nogi, "Marangoni convection and weld shape variations in Ar-O2 and Ar-CO2 shielded GTA welding," *Materials Science and Engineering A*, vol. 380, no. 1, pp. 290–297, 2004.

[16] Y. L. Xu, Z. B. Dong, Y. H. Wei, and C. L. Yang, "Marangoni convection and weld shape variation in A-TIG welding process," *Theoretical and Applied Fracture Mechanics*, vol. 48, no. 2, pp. 178–186, 2007.

[17] K.-H. Tseng and K.-L. Chen, "Comparisons Between TiO2- and SiO2-Flux Assisted TIG Welding Processes," *Journal of Nanoscience and Nanotechnology*, vol. 12, no. 8, pp. 6359–6367, 2012.

[18] E. Ahmadi and A. R. Ebrahimi, "Welding of 316L Austenitic Stainless Steel with Activated Tungsten Inert Gas Process," *Journal of Materials Engineering and Performance*, vol. 24, no. 2, pp. 1065–1071, 2014.

[19] R. S. Vidyarthy, A. Kulkarni, and D. K. Dwivedi, "Study of microstructure and mechanical property relationships of A-TIG welded P91–316L dissimilar steel joint," *Materials Science and Engineering: A*, vol. 695, pp. 249–257, May 2017.

[20] J. J. Vora and V. J. Badheka, "Experimental investigation on mechanism and weld morphology of activated TIG welded bead-on-plate weldments of reduced activation ferritic/martensitic steel using oxide fluxes," *Journal of Manufacturing Processes*, vol. 20, pp. 224–233, 2015.

[21] R. Nakhaei, A. Khodabandeh, and H. Najafi, "Effect of Active Gas on Weld Shape and Microstructure of Advanced A-TIG-Welded Stainless Steel," *Acta Metallurgica Sinica (English Letters)*, pp. 2–7, 2016.

[22] D. J. K. John C. Lippold, “Welding Metallurgy and Weldability of Stainless Steels,” *Wiley Interscience*, p. Book, 2005.